Spatial Sampling Artifacts of Focused Sources in Wave Field Synthesis

Sascha Spors and Jens Ahrens

Deutsche Telekom Laboratories, Technische Universität Berlin, Ernst-Reuter-Platz 7, 10587 Berlin, Germany
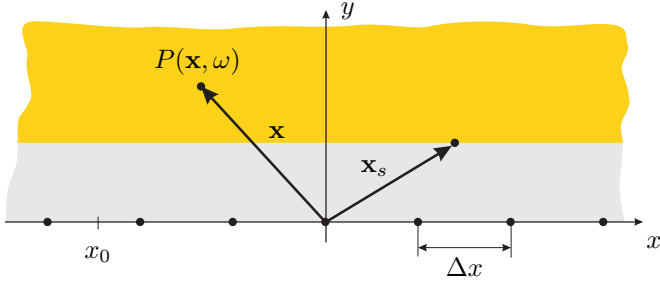
Email: Sascha.Spors@telekom.de

Figure 1: Geometry used to derive the sampling artifacts of focused sources.

Introduction

Wave field synthesis (WFS) is a spatial sound reproduction technique that facilitates a high number of loudspeakers to create a virtual auditory scene. Amongst other interesting properties, WFS allows to reproduce virtual sources that can be positioned in the area between the loudspeakers and the listener. These are known as focussed sources. The physical properties of focussed sources have not been investigated in detail so far. Of special interest in the context of this contribution is the influence of spatial sampling as performed by using discrete loudspeakers in practical implementations. Recently, the properties of virtual point sources reproduced by WFS have been investigated [1]. This paper will serve as a basis for the investigation of the properties of focused sources.

Wave Field Synthesis

Typical implementations of WFS systems are restricted to the reproduction in a plane only using (piecewise) linear loudspeaker arrays. The theoretical basis for this situation is given by the two-dimensional Rayleigh I integral [2, 3]. The Rayleigh I integral states that a linear distribution of monopole line sources (secondary sources) is capable of reproducing a desired wave field (virtual source) in one of the half planes defined by the linear distribution. The wave field in the other half plane is a mirrored version of the desired wave field.

Without loss of generality the geometry depicted in Fig. 1 is assumed: A linear secondary source distribution which is located on the x-axis ($y = 0$) of a Cartesian coordinate system. The reproduced wave field is given by specializing the two-dimensional Rayleigh I integral [4]

$$P(\mathbf{x}, \omega) = -\int_{-\infty}^{\infty} D(\mathbf{x}_0, \omega) G(\mathbf{x} - \mathbf{x}_0, \omega) dx_0 , \quad (1)$$

where $\mathbf{x} = [x\,y]^T$ with $y > 0$ and $\mathbf{x}_0 = [x_0\,0]^T$. The functions $D(\mathbf{x}_0, \omega)$ and $G(\mathbf{x} - \mathbf{x}_0, \omega)$ denote the (secondary source) driving function and the wave field

of the secondary sources, respectively. The secondary source driving function is given as

$$D(\mathbf{x}_0, \omega) = 2\frac{\partial}{\partial \mathbf{n}} S(\mathbf{x}, \omega)\Big|_{\mathbf{x}=\mathbf{x}_0} , \quad (2)$$

where $\frac{\partial}{\partial \mathbf{n}}$ denotes the directional gradient with $\mathbf{n} = [0\,1]^T$ and $S(\mathbf{x}, \omega)$ the wave field of the virtual source. For two-dimensional reproduction the wave field of the secondary sources is given by the two-dimensional free-field Green's function

$$G(\mathbf{x} - \mathbf{x}_0, \omega) = \frac{j}{4} H_0^{(2)}(\frac{\omega}{c}\,|\mathbf{x} - \mathbf{x}_0|) , \quad (3)$$

where $H_0^{(2)}(\cdot)$ denotes the Hankel function of second kind and zeroth-order. Equation (3) can be interpreted as the field of a line source intersecting the listening area at the position $\mathbf{x}_0$.

We will rely on the theory of two-dimensional WFS for the derivation of the sampling artifacts in the spatial frequency domain. Practical implementations of WFS systems use closed loudspeakers as secondary sources. These approximately have the characteristics of acoustic point sources. This mismatch in source types may produce various artifacts in the reproduced wave field that can only be corrected to some extend [3]. This technique is referred to as 2.5D WFS.

Driving Function for Focused Sources

We aim at investigating the spatial sampling artifacts for a focused source with focus point $\mathbf{x}_s$ (see Fig. 1). Various methods exist to derive the required driving signals. In seismic exploration or medical imaging typically the principle of time-delay law focusing or more generally the principle of time-reversal acoustic focusing [5] is used.

In WFS, typically an acoustic sink placed within the listening area is model as desired virtual source. The field of an sink which has equivalent spatial characteristics as a line source is given as [4]

$$S(\mathbf{x}, \omega) = \frac{j}{4} H_0^{(1)}(\frac{\omega}{c}\,|\mathbf{x} - \mathbf{x}_s|) , \quad (4)$$

where $\mathbf{x}_s = [x_s\,y_s]^T$ denotes the position of the focused source with $y_s > 0$. Introducing (4) into (2) results in the driving function for the focused source. This procedure can be regarded as the two-dimensional analogon to time-delay law focusing.

However, the driving function for a focused source will not result in the reproduction of an acoustic sink for the entire listening area. This is due to the fact that the

secondary sources emit wave fields that travel into the listening area. They are driven such that they create a wave field that converges towards the focus point $\mathbf{x}_s$ (gray area in Fig. 1). After the focus point the field diverges again like a point source located at the focus point (yellow area in Fig. 1). Hence, the auralization of a focused point source is only correct if the focused source is located between the secondary sources and the listener. In the context of WFS, this is a well known limitation of focused sources [6].

Spatio Temporal Frequency Domain Description

The reproduced wave field is given, accordingly to Eq. (1) and (3), as a convolution along the x-axis. Applying a spatial Fourier transformation to Eq. (1) with respect to the x-coordinate results in

$$\tilde{P}(k_x, y, \omega) = -\tilde{D}(k_x, \omega)\,\tilde{G}(k_x, y, \omega)\;, \qquad (5)$$

where k_x denotes the spatial frequency (wave number). Spatial frequency domain quantities are denoted by a tilde over the respective variable. The spatial Fourier transform of the driving function and the secondary source are derived in the following.

The spatial Fourier transformation of the secondary sources $\tilde{G}(k_x, y, \omega)$ is given by [1]

$$\tilde{G}(k_x, y, \omega) = \begin{cases} \dfrac{j}{2}\dfrac{e^{-j\sqrt{(\frac{\omega}{c})^2 - k_x^2}\,y}}{\sqrt{(\frac{\omega}{c})^2 - k_x^2}} & \text{for } |k_x| < \left|\frac{\omega}{c}\right|\;, \\ -\dfrac{1}{2}\dfrac{e^{-\sqrt{k_x^2 - (\frac{\omega}{c})^2}\,y}}{\sqrt{k_x^2 - (\frac{\omega}{c})^2}} & \text{for } \left|\frac{\omega}{c}\right| < |k_x|\;, \end{cases} \qquad (6)$$

which is valid for $y > 0$. The spectrum $\tilde{G}(k_x, y, \omega)$ consists of two contributions: a traveling wave contribution for $|k_x| < \left|\frac{\omega}{c}\right|$ and an evanescent contribution for $\left|\frac{\omega}{c}\right| < |k_x|$.

For the considered geometry, the spatial spectrum of the driving function can be computed by exploiting the symmetry of the involved functions, applying suitable substitutions and using the integrals [7, 6.677-3/4]. This results in

$$\tilde{D}(k_x, \omega) = -e^{jk_x x_s}\begin{cases} e^{-j\sqrt{(\frac{\omega}{c})^2 - k_x^2}\,y_s} & \text{for } |k_x| < \left|\frac{\omega}{c}\right|\;, \\ e^{\sqrt{k_x^2 - (\frac{\omega}{c})^2}\,y_s} & \text{for } \left|\frac{\omega}{c}\right| < |k_x|\;, \end{cases} \qquad (7)$$

As for the spectrum of the secondary sources (6), the spectrum of the driving function (7) consists of a propagating and an evanescent part. Note, that the absolute value of $\tilde{D}(k_x, \omega)$ is constant within $|k_x| < \left|\frac{\omega}{c}\right|$.

The reproduced wave field for a focused line source is given by introducing (6) and (7) into (5).

Practical implementations of WFS will always be based on spatially discrete secondary sources. This constitutes a spatial sampling of the continuous secondary source distribution.

Spatial Sampling of Secondary Source Distribution

The discretization of the secondary source distribution is modeled by spatial sampling of the driving function. This is performed by multiplying $D(x, \omega)$ with a series of spatial Dirac functions at the positions of the loudspeakers. For an equidistant spacing this reads

$$D_S(x, \omega) = D(x, \omega) \cdot \frac{1}{\Delta x}\sum_{\mu=-\infty}^{\infty}\delta(x - \Delta x \mu)\;, \qquad (8)$$

where $D_S(x, \omega)$ denotes the sampled driving function and Δx the distance (sampling period) between the sampling positions (indicated by the dots ● in Fig. 1). Applying a spatial Fourier transformation to (8) results in

$$\tilde{D}_S(k_x, \omega) = 2\pi\sum_{\eta=-\infty}^{\infty}\tilde{D}\left(k_x - \frac{2\pi}{\Delta x}\eta, \omega\right)\;. \qquad (9)$$

Equation (9) states that the spectrum $\tilde{D}_S(k_x, \omega)$ of the sampled driving function is given as a superposition of the shifted continuous spectrums $\tilde{D}(k_x - \frac{2\pi}{\Delta x}\eta, \omega)$ of the driving function. Introducing the spectrum of the sampled driving function $\tilde{D}_S(k_x, \omega)$ into (5) results in the spectrum $\tilde{P}_S(k_x, y, \omega)$ of the wave field reproduced by a spatially discrete secondary source distribution. Figure 2 illustrates on a qualitative level the calculation of the reproduced wave field. Qualitatively, artifacts due to the secondary source sampling can be expected when (1) the spectrum of the driving function is not band-limited, and (2) the spectrum of the secondary sources is not band-limited. The first condition ensures that there exists a sampling interval Δx where no spectral overlaps occur in the sampled driving function, the second condition ensures that the spectral repetitions in the sampled driving function will be filtered out by the characteristics of the secondary sources.

Inspection of (6) and (7) reveals that both the spectrum of the driving function and the secondary source are not strictly bandlimited for a given frequency ω due to their evanescent contributions. These contributions decay rapidly, except for low frequencies and/or short distances y to the secondary source distribution. When considering only the propagating part of the driving function the following anti-aliasing condition can be derived

$$f_{\text{al}} \leq \frac{c}{2\Delta x}\;. \qquad (10)$$

Properties of Focused Sources

In order to illustrate the properties of focused sources, the frequency domain description of the reproduced wave field is used for numerical simulations. The spectrum of the reproduced wave field for a sampled secondary source distribution is given by introducing the spectrum of the driving function (7) together with (9) and (6) into (5). The reproduced wave field is given by evaluating the spectral repetitions of the driving function for all η. Figure 3(a) shows the reproduced wave field for
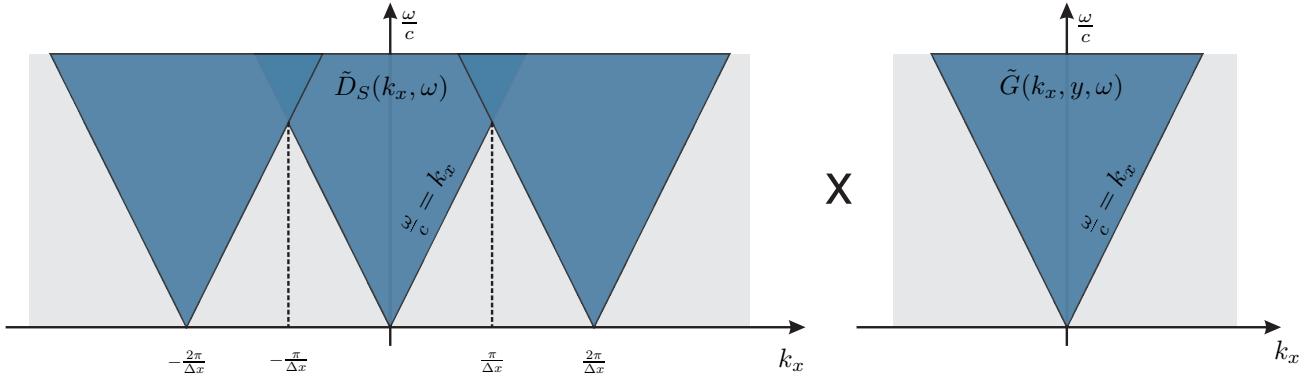
Figure 2: Qualitative illustration of the computation of the spectrum of the reproduced wave field $\tilde{P}_S(k_x, y, \omega)$ for a sampled secondary source distribution.
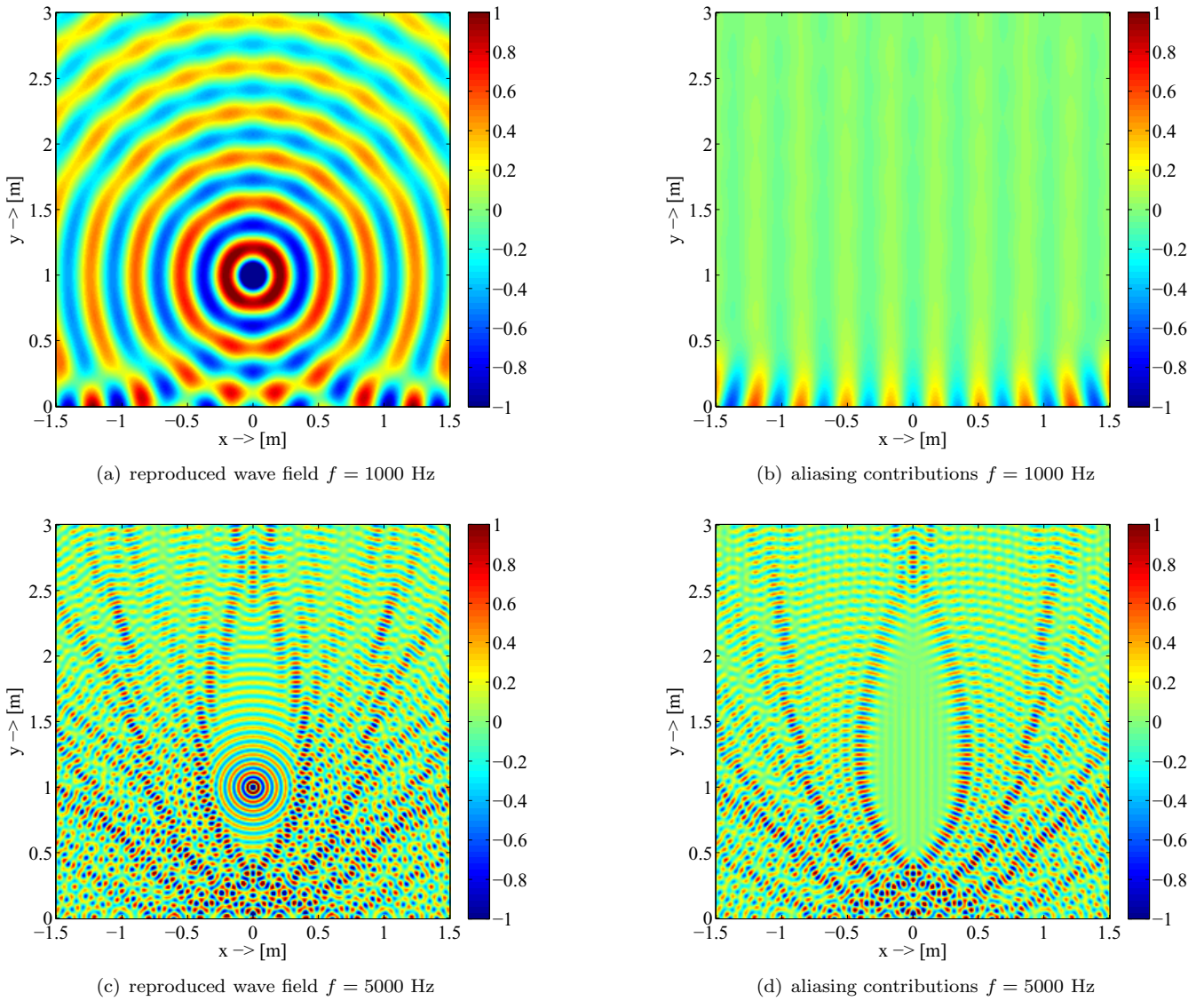

(a) reproduced wave field $f = 1000$ Hz

(b) aliasing contributions $f = 1000$ Hz

(c) reproduced wave field $f = 5000$ Hz

(d) aliasing contributions $f = 5000$ Hz

Figure 3: Reproduced wave field and its aliasing contributions for the reproduction of a monochromatic focused source ($\mathbf{x}_\mathrm{s} = [0\ 1]$ m, $\Delta x = 0.20$ m, 2D WFS).
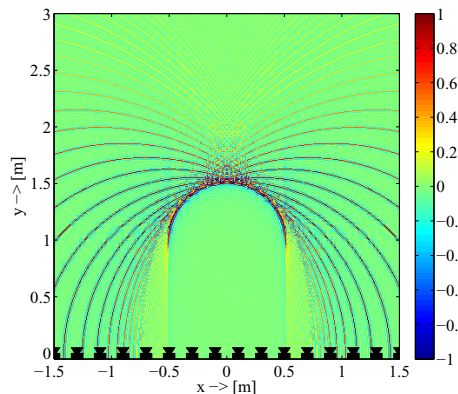
Figure 4: Reproduced wave field for the reproduction of a temporally bandlimited focused source ($b = 20$ kHz, $\mathbf{x}_s = [0\ 1]$ m, $\Delta x = 0.20$ m, $N = 250$, 2.5D WFS)

Figure 5: Impulse response at position $\mathbf{x} = [10\ 2]$ m ($\mathbf{x}_s = [0\ 1]$ m, $\Delta x = 0.20$ m, $N = 250$, 2.5D WFS).

a focused source at position $\mathbf{x}_s = [0\ 1]$ m emitting a monochromatic signal with frequency $f = 1$ kHz. The focus point is clearly visible at the desired position. When animating the wave field (not shown here) it can be observed that the wave fronts converge below the focus point ($y < y_s$) towards the focus point and diverge above. Hence, the desired impression of a point source placed at the position $\mathbf{x}_s$ is only archived above the focus point. Furthermore, a phase shift of 180 degrees can be observed when following the wave field parallel to the y-axis through the focus point (for $x = x_s$). The artifacts visible above the focus point in Fig. 3(a) are due to the limited listening area of focused sources (spatial truncation artifacts). The contributions caused by the sampling of the driving function can be derived by calculating the reproduced wave field for the spectral repetitions ($\eta \neq 0$) only. The resulting wave field is shown in Fig. 3(b). Near field effects are visible close to the loudspeakers, however only slight aliasing artifacts are visible. The anti-aliasing frequency (10) for the simulated scenario is $f_{al} \approx 860$ Hz. Refer to [1] for an analysis of spatial sampling and near field effects in the context of virtual point sources.

The situation changes when increasing the frequency of the focused source. Figures 3(c) and 3(d) show the reproduced wave field and its aliasing contributions for $f = 5$ kHz. Prominent aliasing artifacts are now visible. However, in the vicinity of the focus point these aliasing artifacts degrease leaving the focus point (almost) free of spatial aliasing. This is a very remarkable property of focused sources, which is based on the fact that at the focus point the wave fields emitted by the individual secondary sources superimpose with equal phase. Qualitatively, this also explains the shape of this area. Its size further decreases with increasing frequency. Further time-domain simulations of 2.5D WFS have been performed, in order to derive the properties of focused sources for the emission of broadband signals. Figure 4 shows a temporal snapshot of the resulting wave field (spatio-temporal impulse response) for a typical audio bandwidth of $b = 20$ kHz of the emitted pulse. Aliasing artifacts in the form of additional wave fronts are clearly visible. Interestingly, these artifacts appear before the
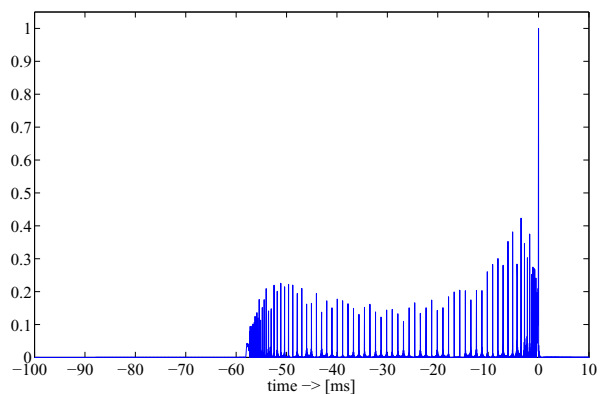
first wavefront of the focused source. This is due to the time-reversal nature of acoustic focusing. For a virtual point source these artifacts would be behind the first wave front. Figure 5 shows the resulting impulse response for one fixed listener position. It can be concluded from Fig. 4 and 5 that the spatial aliasing artifacts for broadband signals result in pre-echos. The temporal extension of these depends on the position of the virtual source and listener, the loudspeaker distance and the total length of the loudspeaker array. Figure 5 shows a rather extreme situation. The simulated geometry is similar to an existing WFS system where these artifacts where clearly audible.

The derived properties have a potential influence on the perception of focused sources. The listener position dependent abrupt change from an (almost) spatial aliasing free zone to a zone with prominent spatial aliasing artifacts will have impact on the perception of moving focused sources or for moving listeners. The pre-echo artifacts have already shown to be audible under certain circumstances. Further subjective experiments will be carried out in the future.

References

[1] S. Spors and J. Ahrens. Spatial aliasing artifacts of wave field synthesis for the reproduction of virtual point sources. In *126th AES Convention*, Munich, Germany, April 2009. Audio Engineering Society (AES).

[2] A.J. Berkhout, D. de Vries, and P. Vogel. Acoustic control by wave field synthesis. *Journal of the Acoustic Society of America*, 93(5):2764–2778, May 1993.

[3] S. Spors, R. Rabenstein, and J. Ahrens. The theory of wave field synthesis revisited. In *124th AES Convention*, Amsterdam, The Netherlands, May 2008. Audio Engineering Society (AES).

[4] E.G. Williams. *Fourier Acoustics: Sound Radiation and Nearfield Acoustical Holography*. Academic Press, 1999.

[5] S. Yon, M. Tanter, and M. Fink. Sound focusing in rooms: the time-reversal approach. *Journal of the Acoustical Society of America*, 113(3):1533–1543, March 2003.

[6] E.N.G. Verheijen. *Sound Reproduction by Wave Field Synthesis*. PhD thesis, Delft University of Technology, 1997.

[7] I.S. Gradshteyn and I.M. Ryzhik. *Tables of Integrals, Series, and Products*. Academic Press, 2000.